HiGANCNN: A Hybrid Generative Adversarial Network and Convolutional Neural Network for Glaucoma Detection

Fairouz Alsulami*, Hind Alseleahbi*, Rawan Alsaedi*, Rasha Almaghdawi*, Tarik Alafif*, Mohammad Ikram*, Weiwei Zong**, Yahya Alzahrani***, and Ahmed Bawazeer****

*Computer Science Department, Jamoum University College, Umm Al-Qura University, Jamoum, Saudi Arabia
{437026993, 436026438, 437018528, 437002552}@st.uqu.edu.sa, tkafif @uqu.edu.sa maikram@uqu.edu.sa
**WeCare.WeTeach, Tory, Michigan, USA, wecare.weteach@gmail.com
***Academic Affairs and Training, Secuirty Forces Hospital, Makkah, Saudi Arabia, yalhasani@sfhm.med.sa
****Department of Ophthalmology, Faculty of medicine, King Abdulaziz University, Jeddah, Saudi Arabia
abawazeer@kau.edu.sa

Abstract

Glaucoma is a chronic neuropathy that affects the optic nerve which can lead to blindness. The detection and prediction of glaucoma become possible using deep neural networks. However, the detection performance relies on the availability of a large number of data. Therefore, we propose different frameworks, including a hybrid of a generative adversarial network and a convolutional neural network to automate and increase the performance of glaucoma detection. The proposed frameworks are evaluated using five public glaucoma datasets. The framework which uses a Deconvolutional Generative Adversarial Network (DCGAN) and a DenseNet pre-trained model achieves 99.6%, 99.08%, 99.4%, 98.69%, and 92.95% of classification accuracy on RIMONE, Drishti-GS, ACRIMA, ORIGA-light, and HRF datasets respectively. Based on the experimental results and evaluation, the proposed framework closely competes with the state-of-the-art methods using the five public glaucoma datasets without requiring any manually preprocessing step.

Keywords:
Glaucoma, Detection, Generative Adversarial Network, K-means, Clustering, Conventional Neural Network.

1. Introduction

GLAUCOMA is an eye disease. It is the second main cause of blindness in the world [1]. It is characterized by cupping of the optic disc with visual field defects secondary to retinal ganglion cell loss. Figure 1 shows glaucoma and non-glaucoma eye images from Drishti-GS dataset. The global number of people with glaucoma is expected to increase to 111.8 million in 2040 [2]. Most cases of Optic nerve damage in glaucoma result from high intraocular pressure. Glaucoma can be detected in the early stages [3]. In late stages, it can lead to complete damage to the optic nerve of the eye [4]. Glaucoma can be diagnosed clinically by medical experts. The medical experts 1 measure Cup-to-disc Ratio (CDR) with parametric identification of visual field defects of the diagnostic techniques to confirm the diagnosis of glaucoma. Kumar et al. [4] showed signs of

glaucoma symptoms. The signs of symptoms include sudden eye pain, headache, nausea, vomiting, blurred and loss of vision. This is why glaucoma is often called the silent thief of vision.
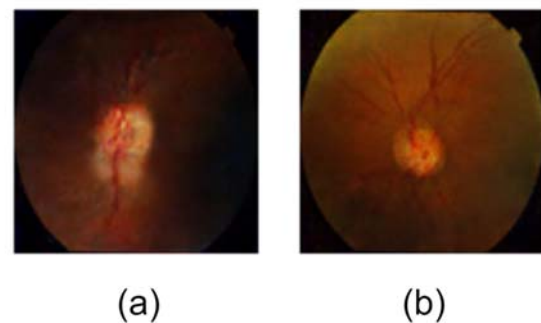

Fig.1 Examples of eye images from Drishti-GS dataset. a) Glaucoma. b) Non-glaucoma.

Kumar et al. [5] showed signs and symptoms of glaucoma. The symptoms may include sudden eye pain, headache, nausea, vomiting, blurred and loss of vision. Most cases are symptomatic. This is why glaucoma is often called the silent thief of vision.

Evidence [4] has shown that clinical detection and prediction of glaucoma is difficult and sensitive in the early stages. It relies on eye medical experts in clinics. The clinical diagnosis is made when the medical expert clinically measures the cup and disc from each image. However, the clinical process is time-consuming which may slow down early detection. Therefore, some efforts have been made for detecting and predicting glaucoma using various techniques of machine and neural networks learning [6].

Convolutional Neural Networks (CNNs) in deep learning have achieved groundbreaking results in the past decade. CNNs have made success in many fields including pattern recognition, voice recognition and image processing [7], disease detection [8], and disease prediction [9], as well as automatic segmentation [10]. The networks have also been widely used in classifying images compared to traditional methods [11].

Recently, Generative Adversarial Networks (GANs) are used successfully in many applications in the computer vision community. The applications include object detection, high-quality image generation [12], and semantic segmentation [13], and speech enhancement [1], and text to photo-realistic image synthesis [14].

GAN [15] is a deep neural network made up of two main networks. The first network is the generator and the other network is the discriminator. The discriminator tries to distinguish the fakeness of the generated images. It can be written as follows:

$$\min_{G} \max_{D} V(G, D)$$

Where

$$\min_{G} \max_{D} V(G, D) = \mathbb{E}_{x \sim p_{data}(x)}[\log D(x)]$$
$$+ \mathbb{E}_{z \sim p_z(z)}[\log(1 - D(G(z)))] \quad (1)$$

The two networks play an opposite game. The generator is trained to produce realistic images while the discriminator is trained to distinguish the real and the generated data. They are both trained simultaneously, and the competition makes the generated images indistinguishable from the real images.

Our work is motivated by the success of Deconvolutional GAN (DCGAN) [16] in image generation without requiring large human efforts of labeling data. The DCGAN adds a CNN to the traditional GAN and improves the quality of the generated images. Also, it has better training stability than the traditional GAN [17].

The remainder of this research work is organized as follows: In **Section 2**, related work is reviewed. In **Section 3**, existing and public glaucoma datasets are described. In **Section 4**, the proposed frameworks for glaucoma detection are presented in detail. In **Section 5**, experimental results and evaluations are provided. Finally, the conclusion and future work are provided in **Section 6**.

2. RELATED WORKS

Many research methods have been applied for glaucoma detection. Some works have used machine learning in addition to image processing techniques while some other methods used deep learning techniques. We briefly describe the current attempts in this research work.

First, Patil et al. [18] applied pre-processing steps and clustering method using a combination of private and public datasets, DRSON-DB, and RIM-ONE, respectively. Then, Al Ghamdi et al. [6] proposed a semi-supervised transfer learning-based method using RIM-ONE dataset to detect early cases of glaucoma. A pre-trained CNN model, VGG-16, was fine-tuned in a supervised manner for a few labeled data. Then, another classifier was used to predict the unlabeled data with the help of the classified labeled data. The authors revealed that self-learning, in which the model teaches itself by training the few unlabeled data to predict the other large part of unlabeled data.

Thakoor et al. [19] used different pre-trained and non-pre-trained CNN models to detect glaucoma. ResNet18, VGG-16, and InceptionNet pre-trained CNN models were used. The pre-trained models were evaluated on a small private dataset. Diaz-Pinto et al. [20] applied a DCGAN and a semi-supervised learning method (SS-DCGAN) using a small number of labeled retinal images to assess glaucoma in semi-supervised learning. The method was evaluated on a combination of fourteen private and public glaucoma datasets.

Followed by [18], [6], [19], and [20], Ovreiu et el. [21] used a densely connected pre-trained CNN model (DenseNet-121) to classify normal and glaucoma images. Datasets such as RIM-ONE and ACRIMA were used. They have shown that the DenseNet-121 model performs better at identifying images of glaucoma in the early stages. Bisneto et al. [22] proposed a conditional GAN (cGAN) based segmentation method to perform the optic disc detection. Features were extracted using a texture descriptor. Drishti-GS and RIM-ONE datasets were used. Then, Multilayer perceptron, Sequential Minimal Optimization, and Random Forest classifiers were employed. Although this method achieves a complete performance, it is computationally and manually exhaustive since it requires many pre-processing steps such as segmentation, texture feature extraction, filling holes for noise removal, and histogram equalization before classification.

Different from the existing works, the proposed framework doesn't require any of the pre-processing steps. The framework combines the DCGAN with the DenseNet-121 pre-trained CNN model for glaucoma detection. The DCGAN generator is used to generate more glaucoma and non-glaucoma images, which feeds the DenseNet classifier for better effectiveness in automating the detection of glaucoma.

3. EXISTING PUBLIC GLAUCOMA DATASETS

In this section, we provide a description of the current public datasets used to screen for glaucoma detection. Table 1 shows statistics of existing public glaucoma datasets. The details of the datasets are described as follows:

Table 1: Statistics of existing public glaucoma datasets.

Dataset	Glaucoma	Normal	Total
RIM-ONE	194	261	455
Drishti-GS	70	31	101
ORIGA-light	168	482	650
HRF	27	18	45
ACRIMA	396	309	705
TOTAL	855	1,101	1,956

RIM-ONE [23]. RIM-ONE is an open retinal fundus images dataset that contains 455 high-resolution images in total. It includes 261 normal images and 194 glaucoma fundus images. These images are developed in collaboration with three Spanish hospitals: Hospital Universitario de Canarias, Hospital Clınico San Carlos, and Hospital Universitario Miguel Servet.

DRISHTI-GS [24]. DRISHTI-GS is another public dataset that includes 101 images in total. It includes 70 Glaucoma images and 31 normal images for diagnosing ocular diseases such as glaucoma.

ORIGA-light [25]. ORIGA-light is a public retinal fundus image dataset. It contains 650 images (168 Glaucoma and 482 normal) for diagnosing ocular diseases such as glaucoma and diabetic retinopathy.

HRF [26]. HRF is a small public dataset. It contains 45 retinal fundus images in total. It includes 18 normal images and 27 Glaucoma images.

ACRIMA [27]. ACRIMA is another public retinal fundus images dataset. It is composed of 705 fundus images (396 glaucoma and 309 normal images). Most of the fundus images in this dataset are captured from the left and right eyes which are dilated and centered in the optic disc.

4. PROPOSED FRAMEWORKS

Our goal in this research is to automate the detection of glaucoma from eye images with higher accuracy. Therefore, we propose three different frameworks to detect glaucoma. Figure 5 shows one of our proposed frameworks with the best performance. The frameworks are as follows:

- K-means with a pre-trained CNN model.

- DCGAN with a pre-trained CNN model.

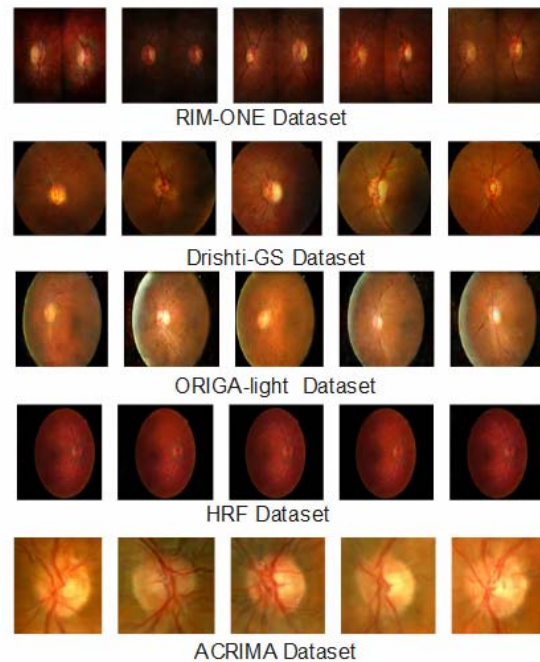- DCGAN and K-means with a pre-trained CNN model.

Fig.2 A sample of the generated images from five public glaucoma datasets.

In the first framework, we apply K-means with a pre-trained CNN model to see whether the clustering and segmentation can affect glaucoma classification. In the second framework, we apply a generative adversarial network, more specifically the DCGAN, in addition to the pre-trained CNN models to generate more images for training the CNN model. In the third framework, we apply Kmeans clustering in addition to the DCGAN and the pre-trained CNN models to see whether clustering and image generation can affect the classification performance.

We fine-tune and apply two pre-trained CNN models that are already trained on ImageNet. The two pre-trained CNN models are applied in all the frameworks. The first model we use is a Dense Convolutional Network (DenseNet-121) [28]. From its name, it consists of 121 layers. The dense layers use the sigmoid activation function to pump the data to other layers.

Fig.3 A sample of the learned kernels for glaucoma and non-glaucoma from the DenseNet-121 model.

The layers are connected and trained using Adam optimizer in a feed-forward and a backpropagation fashion to minimize the loss function. Figure 7 shows the training validations and the loss curves after training the Keras pre-trained DenseNet-121 model using the existing public datasets. The images are resized to 224x224. Image augmentation technique is applied to increase the number and verity of images. Thus, it increases the generalization ability. A batch size of 32 is used. A dropout technique is used to speed up the training. kernels are learned during convolution in the convolutional layers to learn the boundary and the edges from the training samples. In the DenseNet121 model, we use different learned kernel sizes respectively in the convolutional layers. A sample of the learned kernels during the training process is shown in Figure 3.

For each layer, the feature maps in all convolutional layers are used as inputs in the average pooling layers. A sample of feature maps of glaucoma and non-glaucoma-generated images is shown in Figure 4. The feature maps are extracted from the last layer of the DenseNet-121 model. A binary cross entropy function is used to measure the loss.

In addition to the DenseNet-121 model, we apply another pre-trained CNN model, called MobileNet. The MobileNet is another popular pre-trained CNN model released by Google [29]. It contains 30 convolutional layers with Stride2, a deep layer, a bitmap layer with double the number of channels, a deep layer with line 2, bitmap layer with the channel number.

The last layer of the pre-trained models is binary classifiers. The binary classifiers return the value 1 if the eye image is affected by glaucoma and the value -1 otherwise.

We use the DCGAN in the last two frameworks to generate more glaucoma and non-glaucoma images since the number of glaucoma images in the existing public datasets is low. The DCGAN mainly consists of two stages: the learning stage and the generation stage. In the learning

phase, the generator draws samples from an N-dimensional normal distribution that runs through the generator to obtain a synthetic sample while the discriminator attempts to distinguish between images taken from the generator and images from the training set. In the generator, batch normalization and momentum are employed to speed up the learning process and avoid overfitting. A kernel size of 3 is used during the convolutions. We use Rectified Linear Unit (ReLU) and Tangent Hyperbolic (Tanh) activation functions in the generator layers. In the discriminator, we apply dropout, learning rate, momentum, and batch normalization techniques to reduce overfitting and accelerate the training speed. LeakyRelU and Sigmoid activation functions are used. Adam optimizer is employed in both the discriminator and the generator. A cross-entropy function is used to measure the error loss. 6,000 glaucoma and nonglaucoma images are generated for each dataset. Figure 2 shows a sample of the generated images from the existing glaucoma datasets. The generated dataset is available at https://www.kaggle.com/datasets/hindsaud/datasets-higancnn-glaucoma-detection.
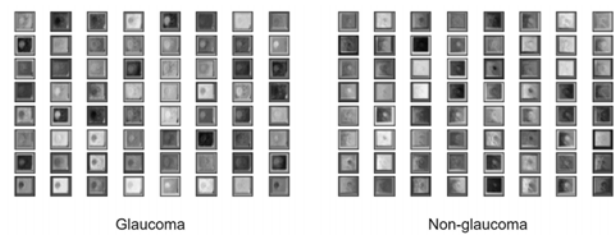

Fig. 4 A sample of feature maps of glaucoma and non-glaucoma generated images. The feature maps are extracted from the last layer from DenseNet-121 trained classifier.
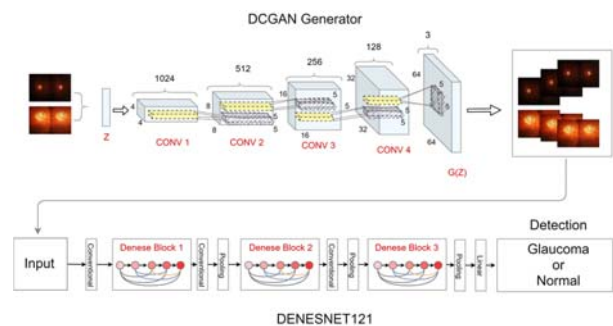

Fig.5 An architecture of our fourth proposed framework for detecting glaucoma using a hybrid of a DCGAN generator and a DenseNet-121 classifier.

Lastly, we apply unsupervised K-means in the last framework. This aims to cluster and segment the eye images to see whether it is normal or infected by glaucoma. The clustering algorithm groups similar features of pixels from

the eye images. The K-means algorithm creates random centroids in each image based on the number of clusters provided. Then, it attempts to fit each data point into the closest centroid. The centroids are adjusted automatically based on the last nearest data point allocated to them. This iterative process continues until all data points are associated with the centroids. Hence, it creates distinct clusters to train the pre-trained CNN models. Figure 6 shows an example of clustered normal and glaucoma images.
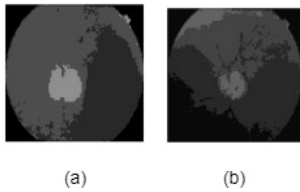

Fig.6 Examples of the clustered normal and glaucoma images using K-means: (a) Glaucoma (b) Non-glaucoma.

Table 2: Comparing the performance of the three proposed frameworks using the existing glaucoma public datasets. The best values are in bald.

Dataset	Pre-trained CNN Model	ACC(%) (K-means + Pre-trained CNN Model, DCGAN + Pre-trained CNN Model, DCGAN + K-means + Pre-trained CNN Model)	Spe(%) (K-means + Pre-trained CNN Model, DCGAN + Pre-trained CNN Model, DCGAN + K-means + Pre-trained CNN Model)	Sen(%) (K-means + Pre-trained CNN Model, DCGAN + Pre-trained CNN Model, DCGAN + K-means + Pre-trained CNN Model)	AUC(%) (K-means + Pre-trained CNN Model, DCGAN + Pre-trained CNN Model, DCGAN + K-means + Pre-trained CNN Model)	Training Speed per second (K-means + Pre-trained CNN Model, DCGAN + Pre-trained CNN Model, DCGAN + K-means + Pre-trained CNN Model)
RIM-ONE	DenseNet-121	93.75 , **99.6**, 98.36	**100**,100, 97	66, 99, **100**	83, 99, 98	240,420, 240
	MobileNet	87.4, 96.8, 99.08	**100**, 93, 99	33, **100**, 98	66, 96, 99	300, 100, 420
HRF	DenseNet-121	60, 92.93, 99.6	50, **100**, 100	66, 86, 99	58.3, 93, **99.6**	180, 300, 180
	MobileNet	80, 94.91, 93.6	**100**, 89, **100**	50, **100**, 18	75, 94, 59	180, 300, 300
ACRIMA	DenseNet-121	91.22, 99.4, 93.46	**100, 100**, 89	86.8, 99, 97	93, 99, 93	180, 180, 490
	MobileNet	86.66, 96.71, 99.08	73, **100**, 99	96.2, 93, 99	84.59, 96.7, 99	240, 180, 420
ORIGA-light	DenseNet-121	75.90, 98.6, 95.16	91.2, 97, 91	42.3, **100**, 98	66.7, 98, 95	200, 300, 240
	MobileNet	72.2, 95.94, 97.9	89.5, 92, 96	34.6, **100**, 99	62, 95, 97	120, 300, 240
DRISHTI-GS	DenseNet-121	61.53, 99.08, 51.0	**100**, 98, 53	44.4, **100**, 69	72, 99, 51	180, 180, 480
	MobileNet	69.23, 99.6, 48.8	50, 99, 78	77, **100**, 18	61, 99, 48	**120, 120**, 180

Table 3: Comparison results with the state-of-the-art methods

Authors	Method	Dataset	Accuracy(%)	AUC(%)	Specificity(%)	Sensitivity(%)
Al Ghamdi et al. [6]	Semi-supervised	RIM-ONE	92.4	83.65	91.7	93.3
Bisneto et al. [12]	cGAN and taxonomic diversity indexes	RIM-ONE and DRISHTI-GS	100	100	100	100
Diaz-Pinto et al. [10]	DCGAN and SS-DCGAN	Fourteen private and public datasets including RIM-ONE, HRF, ACRIMA, ORIGA-light, and DRISHTI-GS	-	90.17	79.86	82.90
Ovreiu et al. [11]	DenseNet-121	RIM-ONE and HRF	95.6	97.1	98.8	95.2
Al Bander et al. [10]	CNN and SVM	RIM-ONE	88.2	-	90.8	85
Ours	DCGAN and DenseNet-121	RIM-ONE	99.6	99	100	99.2
		HRF	92.93	93	100	86
		ACRIMA	99.4	99	100	99
		ORIGA-light	98.69	98	97	100
		Drishti-GS	99.08	99	98	100

5. EXPERIMENTS

In this section, we first provide implementation details for training and testing the proposed frameworks. Second, we compare the performance of the frameworks. Then, we evaluate our best performance framework against all published methods using the existing public datasets, RIM-ONE HRF, ACRIMA, ORIGA-light, and DRISHTI-GS. Each dataset is randomly split into 85% for training and 15% for testing.

Implementation. Our various experiments for the frameworks were performed on a GPU. We used Google Colaboratory (Colab) and Keras 3.4.3 with TensorFlow 2 [31] to implement the four frameworks. A python programming language version 3.7 was used.

Experimental Results and evaluation. We use the public benchmark datasets, RIM-ONE, HRF, ACRIMA, ORIGA-light, and DRISHTI-GS to compare the performance of the four proposed frameworks. The accuracy, specificity, sensitivity, and Area Under the Curve (AUC) for the frameworks are computed. The AUC is used to compute the area under the Receiver Operating Characteristic (ROC) curve and compare the performance of the classifiers. Then, the accuracy, specificity, and sensitivity are computed as follows:

$$Accuracy = \frac{T_P + T_N}{T_P + F_P + F_N + T_N} \qquad (1)$$

$$Specificity = \frac{T_N}{T_N + F_P} \qquad (2)$$

$$Sensitivity = \frac{T_P}{T_P + F_N} \qquad (3)$$

Measuring the eye-generated images. To measure the realness and fakeness of the generated images by the DCGAN, we use Frechet Inception Distance (FID) metric [32] on the five public glaucoma datasets. The less value is the better result in discriminating the realness and fakeness of the generated images. From Table 4, we attain the best result using the RIM-ONE dataset.
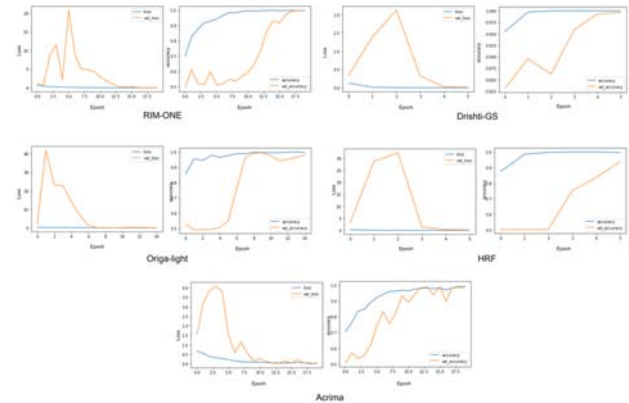

Fig. 7. The training validations and the loss curves after training the Keras pre-trained DenseNet-121 model using the existing public datasets.

Comparing the performance of the three proposed frameworks. We evaluate the frameworks among themselves to measure their efficiency and effectiveness. As shown in Table 2, the DCGAN with pre-trained DenseNet-121 framework achieves higher detection accuracy of 96.6% compared to other frameworks using ACRIMA dataset. On the other hand, the DCGAN and K-means with the pre-trained DenseNet-121 framework

achieves a better AUC of 99.6% compared to other frameworks using HRF dataset. The ROC curves for the DenseNet-121 classifier using the existing public datasets are depicted in Figure 8. Complete specificities and sensitivities vary among the frameworks. To compare the speed of the frameworks, the K-means and the DCGAN frameworks using the pre-trained MobileNet model achieve less training times with 120 seconds using the DRISHTI-GS dataset.
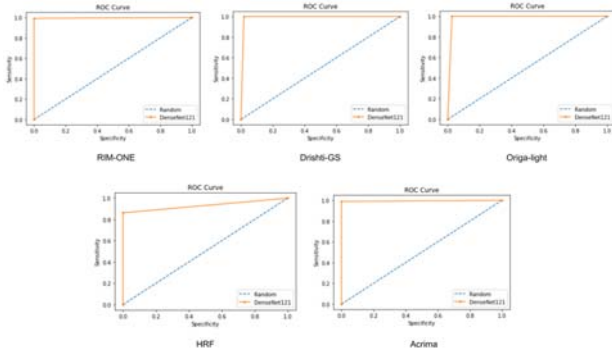

Fig. 8. The ROC curves for the DenseNet-121 classifier using the existing public datasets.

Table 4 FID evaluations on the generated images using the DCGAN. The best values are in bald.

	FID	
Dataset	Glaucoma	Normal
RIM-ONE	**337.7**	**342.6**
Drishti-GS	389.75	455.17
ORIGA-light	379.35	370.84
HRF	404	393.29
ACRIMA	409.36	394.22

Comparison with the state-of-the-art (SOTA) methods. We use RIM-ONE, Drishti-GS, ACRIMA, ORIGA-light, and HRF to evaluate our best performance framework, DCGAN and DenseNet121, against all published methods. As shown in Table 3, the DCGAN with the DenseNet-121 framework achieves high accuracy and AUC compared to the state-of-the-art methods using the five public datasets. It closely competes with work in [22]. Compared to [22], our framework doesn't require any manual processing step.

6. CONCLUSION

Due to the lack of glaucoma data, in this research, we propose different frameworks, including a hybrid of a generative adversarial network and a convolutional neural network to automate and increase the performance for

glaucoma detection. The proposed frameworks are evaluated using five public glaucoma datasets. The framework which uses the Deconvolutional Generative Adversarial Network (DCGAN) and the DenseNet-121 pre-trained model achieves 99.6%, 99.08%, 99.4%, 98.69%, and 92.95% of classification accuracy on RIM-ONE, Drishti-GS, ACRIMA, ORIGA-light, and HRF datasets respectively. Based on the experimental results and evaluation, the proposed framework closely competes with the state-of-the-art methods using the five public glaucoma datasets without requiring any manually pre-processing step. The image generation and transfer learning applied in this work has demonstrated the effectiveness in glaucoma detection when few labeled images are available. In the future, we will involve an attention mechanism to attain higher performance in the detection of glaucoma.

References

[1] S. Pascual, A. Bonafonte, and J. Serra, "Segan: Speech enhancement generative adversarial network," arXiv preprint arXiv:1703.09452, 2017.

[2] Y.-C. Tham, X. Li, T. Y. Wong, H. A. Quigley, T. Aung, and C.-Y. Cheng, "Global prevalence of glaucoma and projections of glaucoma burden through 2040: a systematic review and meta-analysis," Ophthalmology, vol. 121, no. 11, pp. 2081–2090, 2014.

[3] M. Aouf, S. Almotatiri, A. Bajahzar, and G. Kareem, "Glaucoma detection from fundus camera image," in 2019 Ninth International Conference on Intelligent Computing and Information Systems (ICICIS). IEEE, 2019, pp. 312–316.

[4] T. Khalil, S. Khalid, and A. M. Syed, "Review of machine learning techniques for glaucoma detection and prediction," in 2014 Science and Information Conference. IEEE, 2014, pp. 438–442.

[5] B. N. Kumar, R. Chauhan, and N. Dahiya, "Detection of glaucoma using image processing techniques: A review," in 2016 International Conference on Microelectronics, Computing and Communications (MicroCom). IEEE, 2016, pp. 1–6.

[6] M. Al Ghamdi, M. Li, M. Abdel-Mottaleb, and M. Abou Shousha, "Semi-supervised transfer learning for convolutional neural networks for glaucoma detection," in ICASSP 2019-2019 IEEE International Conference on Acoustics, Speech and Signal Processing (ICASSP). IEEE, 2019, pp. 3812–3816.

[7] S. Albawi, T. A. Mohammed, and S. Al-Zawi, "Understanding of a convolutional neural network," in 2017 International Conference on Engineering and Technology (ICET), 2017, pp. 1–6.

[8] L. Racˇi c, T. Popoviˊ c, S.ˊ cakiˇ c, and S.ˊ Sandi, "Pneumonia detection using deep learning based on convolutional neural network," in 2021 25th International Conference on Information Technology (IT), 2021, pp. 1–4.

[9] H. Maryam Tavakoli, T. Xie, J. Shi, M. Hadzikadic, and Y. Ge, "Predicting neural deterioration in patients with alzheimer's disease using a convolutional neural network," in

2020 IEEE International Conference on Bioinformatics and Biomedicine (BIBM), 2020, pp. 1951–1958.

[10] N. George and C. V. Jiji, "Convolutional neural network for automatic segmentation of edi oct images," in 2019 10th International Conference on Computing, Communication and Networking Technologies (ICCCNT), 2019, pp. 1–5.

[11] E. Chen, X. Wu, C. Wang, and Y. Du, "Application of improved convolutional neural network in image classification," in 2019 International Conference on Machine Learning, Big Data and Business Intelligence (MLBDBI), 2019, pp. 109–113.

[12] Z. Zhang, X. Pan, S. Jiang, and P. Zhao, "High-quality face image generation based on generative adversarial networks," Journal of Visual Communication and Image Representation, vol. 71, p. 102719, 2020. [Online]. Available: https://www.sciencedirect.com/science/article/pii/S1047320 319303402

[13] W. Chen, T. Zhang, and X. Zhao, "Semantic segmentation using generative adversarial network," in 2021 40th Chinese Control Conference (CCC), 2021, pp. 8492–8495.

[14] H. Zhang, T. Xu, H. Li, S. Zhang, X. Wang, X. Huang, and D. Metaxas, "Stackgan: Text to photo-realistic image synthesis with stacked generative adversarial networks," in 2017 IEEE International Conference on Computer Vision (ICCV), 2017, pp. 5908–5916.

[15] I. Goodfellow, J. Pouget-Abadie, M. Mirza, B. Xu, D. Warde-Farley, S. Ozair, A. Courville, and Y. Bengio, "Generative adversarial nets," Advances in neural information processing systems, vol. 27, 2014.

[16] T. Alkhodidi, L. Aljoudi, A. Fallatah, A. Bashy, N. Ali, N. Alqahtani, N. Almajnooni, A. Allhabi, T. Albarakati, T. Alafif, and S. Sasi, "Geac: Generating and evaluating handwritten Arabic characters using generative adversarial networks," in 2021 International Conference on Computational Intelligence and Knowledge Economy (ICCIKE), 2021, pp. 228–233.

[17] S. Chintala, E. Denton, M. Arjovsky, and M. Mathieu, "How to train a gan? tips and tricks to make gans work," GitHub, Dec, 2016.

[18] D. D. Patil, R. R. Manza, G. C. Bedke, and D. D. Rathod, "Development of primary glaucoma classification technique using optic cup disc ratio," in 2015 International Conference on Pervasive Computing (ICPC), 2015, pp. 1–5.

[19] K. A. Thakoor, X. Li, E. Tsamis, P. Sajda, and D. C. Hood, "Enhancing the accuracy of glaucoma detection from oct probability maps using convolutional neural networks," in 2019 41st Annual International Conference of the IEEE Engineering in Medicine and Biology Society (EMBC). IEEE, 2019, pp. 2036–2040.

[20] A. Diaz-Pinto, A. Colomer, V. Naranjo, S. Morales, Y. Xu, and A. F. Frangi, "Retinal image synthesis and semi-supervised learning for glaucoma assessment," IEEE transactions on medical imaging, vol. 38, no. 9, pp. 2211–2218, 2019.

[21] S. Ovreiu, I. Cristescu, F. Balta, and E. Ovreiu, "An exploratory study for glaucoma detection using densely connected neural networks," in 2020 International Conference on e-Health and Bioengineering (EHB). IEEE, 2020, pp. 1–4.

[22] T. R. V. Bisneto, A. O. de Carvalho Filho, and D. M. V. Magalhaes, "Generative adversarial network and texture features applied to automatic glaucoma detection," Applied Soft Computing, vol. 90, p. 106165, 2020.

[23] F. Fumero, S. Alayon, J. L. Sanchez, J. Sigut, and M. Gonzalez-Hernandez, "Rim-one: An open retinal image database for optic nerve evaluation," in 2011 24th International Symposium on Computer-Based Medical Systems (CBMS), 2011, pp. 1–6.

[24] J. Sivaswamy, S. R. Krishnadas, G. Datt Joshi, M. Jain, and A. U. Syed Tabish, "Drishti-gs: Retinal image dataset for optic nerve head(onh) segmentation," in 2014 IEEE 11th International Symposium on Biomedical Imaging (ISBI), 2014, pp. 53–56.

[25] Z. Zhang, F. S. Yin, J. Liu, W. K. Wong, N. M. Tan, B. H. Lee, J. Cheng, and T. Y. Wong, "Origa-light: An online retinal fundus image database for glaucoma analysis and research," in 2010 Annual International Conference of the IEEE Engineering in Medicine and Biology, 2010, pp. 3065–3068.

[26] "High-resolution fundus (hrf) image database," https://www5.cs.fau.de/ research/data/fundus-images/.

[27] A. Diaz-Pinto, S. Morales, V. Naranjo, T. Kohler, J. M. Mossi, and A. Navea, "Cnns for automatic glaucoma assessment using fundus images: an extensive validation," Biomedical engineering online, vol. 18, no. 1, pp. 1–19, 2019.

[28] O. Rochmawanti and F. Utaminingrum, "Chest x-ray image to classify lung diseases in different resolution size using densenet-121 architectures," in 6th International Conference on Sustainable Information Engineering and Technology 2021, 2021, pp. 327–331.

[29] L. G. Falconı, M. P′erez, and W. G. Aguilar, "Transfer learning in breast′ mammogram abnormalities classification with mobilenet and nasnet," in 2019 International Conference on Systems, Signals and Image Processing (IWSSIP). IEEE, 2019, pp. 109–114.

[30] B. Al-Bander, W. Al-Nuaimy, M. A. Al-Taee, and Y. Zheng, "Automated glaucoma diagnosis using deep learning approach," in 2017 14th International Multi-Conference on Systems, Signals & Devices (SSD). IEEE, 2017, pp. 207–210.

[31] M. Abadi, A. Agarwal, P. Barham, E. Brevdo, Z. Chen, C. Citro, G. S. Corrado, A. Davis, J. Dean, M. Devin, S. Ghemawat, I. Goodfellow, A. Harp, G. Irving, M. Isard, Y. Jia, R. Jozefowicz, L. Kaiser, M. Kudlur, J. Levenberg, D. Mane, R. Monga, S. Moore, D. Murray, C. Olah, M. Schuster, J. Shlens, B. Steiner, I. Sutskever, K. Talwar, P. Tucker, V. Vanhoucke, V. Vasudevan, F. Viegas, O. Vinyals, P. Warden, M. Wattenberg, M. Wicke, Y. Yu, and X. Zheng, "Tensorflow: Large-scale machine learning on heterogeneous distributed systems," arXiv preprint arXiv:1603.04467, 2016.

[32] M. Heusel, H. Ramsauer, T. Unterthiner, B. Nessler, and S. Hochreiter, "Gans trained by a two time-scale update rule converge to a local nash equilibrium," in Advances in neural information processing systems, 2017, pp. 6626–6637.

Fairouz Al-Sulami received her BSc in Computer Science from Jamoum University College, Umm Al-Qura University, Makkah Al-Mukarramah, Saudi Arabia, in 2021. Her research interests include computer vision, machine learning, deep learning, and information systems.

Hind Alseleahbi received her BSc degree in Computer Science from University College in Al Jamoum, Umm Al-Qura University, Makkah, KSA, in 2021. She is currently a Data Engineering Intern in Lean Business Services. Her research interests include computer vision, machine learning, deep learning, and data engineering

Rawan Alsaedi received her BSc degree in Computer Science from Jamoum University College, Umm Al-Qura University in 2021. Her research interests include computer vision, machine learning, and deep learning.

Rasha Al-maghdawi received her Bachelor's degree in Computer Science from Jamoum University College, Umm Al-Qura University in Makkah Al-Mukarramah, Saudi Arabia in 2021, from her research interests in health care and disease diagnosis using artificial intelligence and deep learning techniques.

Dr. Tarik Alafif received his Ph.D. degree from Computer Science Department at Wayne State University, Detroit, MI, US in 2017 and his Master's from Gannon University, Erie, PA, US, in 2011. He is currently an Assistant Professor in the Computer Science Department at Jamoum University College of Umm Al-Qura University. His main research interest includes Computer Vision, Machine and Deep Learning, and Large-scale Data. He has published many peer-reviewed papers in these areas in prestigious international conferences and journals.

Dr. Mohammed Ikram received his Ph.D. degree from the school of computer science department at the University of Technology Sydney, Australia in 2020 and his masters from the same university in 2015. His research interests include, but are not limited to Cloud Computing, networking systems, and data science. He is currently working as an Assistant Professor in the school of computer science, Jamoum University College at Umm Al-Qura University.

Dr. Weiwei Zong received her bachelor's degree in information security from Central South University, China in 2008; and her Ph.D. in machine learning from Nanyang Technological University, Singapore in 2013. Her research interests include but are not limited to deep learning, machine learning, computer vision, medical data, etc. She now is pitching for her startup WeCare.WeTeach as the CEO & Co-founder, which aims to benefit large groups of community members including students, patients, medical practitioners, and many more.

Dr. Yahya Alzahrani

Dr. Ahmad Bawazeer